Neuron
Report

A Major Role for Intracortical Circuits in the Strength and Tuning of Odor-Evoked Excitation in Olfactory Cortex

Cindy Poo[1] and Jeffry S. Isaacson[1,*]
[1]Center for Neural Circuits and Behavior, Department of Neuroscience, School of Medicine, University of California, San Diego, 9500 Gilman Drive, La Jolla, CA 92093, USA
*Correspondence: jisaacson@ucsd.edu
DOI 10.1016/j.neuron.2011.08.015

SUMMARY

In primary sensory cortices, there are two main sources of excitation: afferent sensory input relayed from the periphery and recurrent intracortical input. Untangling the functional roles of these two excitatory pathways is fundamental for understanding how cortical neurons process sensory stimuli. Odor representations in the primary olfactory (piriform) cortex depend on excitatory sensory afferents from the olfactory bulb. However, piriform cortex pyramidal cells also receive dense intracortical excitatory connections, and the relative contribution of these two pathways to odor responses is unclear. Using a combination of in vivo whole-cell voltage-clamp recording and selective synaptic silencing, we show that the recruitment of intracortical input, rather than olfactory bulb input, largely determines the strength of odor-evoked excitatory synaptic transmission in rat piriform cortical neurons. Furthermore, we find that intracortical synapses dominate odor-evoked excitatory transmission in broadly tuned neurons, whereas bulbar synapses dominate excitatory synaptic responses in more narrowly tuned neurons.

INTRODUCTION

In the olfactory bulb, odors activate stereotyped and distinct sets of glomeruli, and the output of mitral/tufted (M/T) cells belonging to individual glomeruli encodes odorant molecular features (Rubin and Katz, 1999; Soucy et al., 2009; Uchida et al., 2000; Wachowiak and Cohen, 2001). M/T cell axons project via the lateral olfactory tract (LOT) to the piriform cortex, a three-layered cortical region where bulbar inputs are integrated to form odor percepts (Haberly, 2001). Within the piriform cortex, layer 2/3 pyramidal cells receive direct sensory input from M/T cells on their apical dendrites. Whereas olfactory information is encoded as a spatial map of activated M/T cells in the olfactory bulb, odor representations in layer 2/3 of the piriform cortex are distributed among spatially dispersed cell ensembles and lack stereotypy (Illig and Haberly, 2003; Rennaker et al., 2007; Stettler and Axel, 2009). The mechanisms governing this transformation from a spatially segregated representation in the olfactory bulb to one that is highly distributed and nonstereotyped in the cortex are not well understood.

Individual pyramidal cells in the piriform cortex are thought to receive converging input from M/T cells belonging to different glomeruli (Apicella et al., 2010; Davison and Ehlers, 2011; Miyamichi et al., 2011; Wilson, 2001), and M/T cell axons from individual glomeruli project diffusely throughout the piriform cortex without obvious spatial patterning (Ghosh et al., 2011; Sosulski et al., 2011). Although it is tempting to account for cortical odor responses entirely by the convergence and divergence of direct olfactory bulb inputs, the dendrites of the piriform cortex pyramidal cells also receive extensive intracortical associational (ASSN) connections from excitatory neurons within the piriform cortex and other cortical regions (Haberly, 2001; Haberly and Price, 1978; Johnson et al., 2000). Although much effort has focused on elucidating how olfactory bulb afferent sensory inputs shape cortical odor representations, the contribution of intracortical excitatory circuits to odor responses has been largely unexplored.

In this study, we examine the relative contributions of sensory afferent input and intracortical connections to odor-driven excitatory synaptic transmission in the anterior piriform cortex (APC). We take advantage of the differential expression of presynaptic $GABA_B$ receptors in APC to selectively silence intracortical synapses while leaving afferent sensory fibers unaffected. We show that intracortical connections in APC underlie the strength of odor-evoked excitatory synaptic transmission and expand the range of odors over which pyramidal cells can respond. Our results indicate that intracortical ASSN circuits make a major contribution to odor-evoked excitation, suggesting that odor representations in the piriform cortex cannot simply be accounted for by the convergence and divergence of M/T cell inputs.

RESULTS

Selective Silencing of Intracortical ASSN Synaptic Input In Vivo

$GABA_B$ receptors are expressed on nerve terminals, and activation of presynaptic $GABA_B$ receptors causes a potent inhibition of neurotransmitter release from both pyramidal cells and local

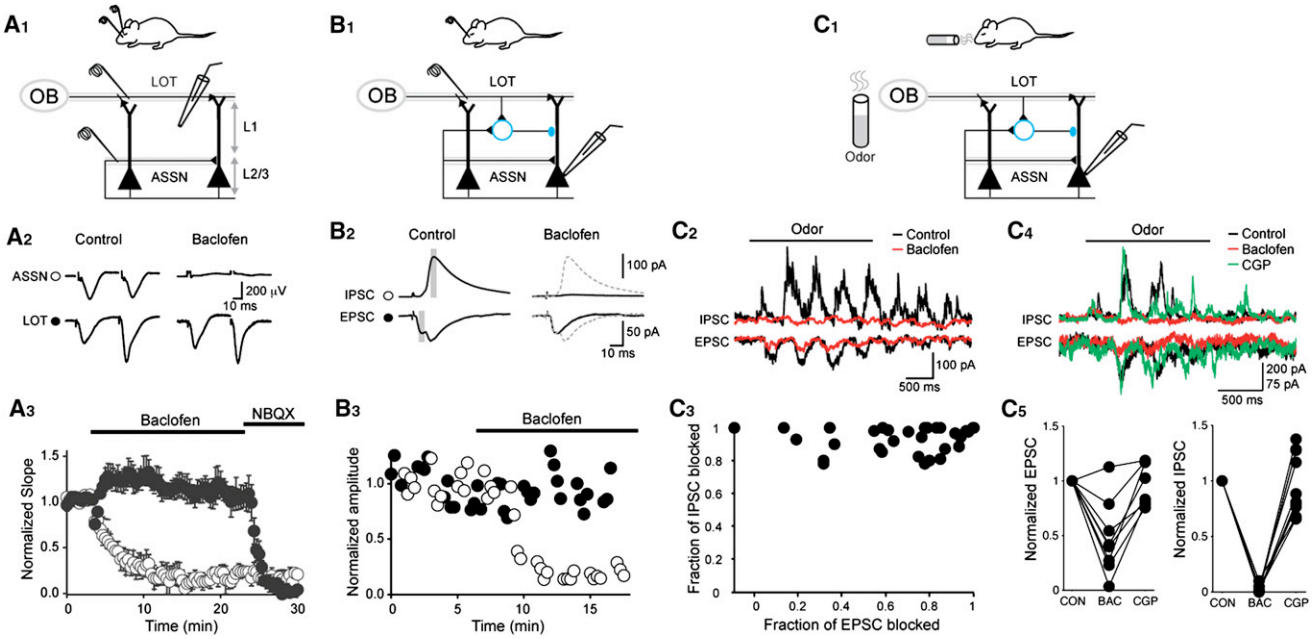

Figure 1. Selective Silencing of Intracortical Excitation in Rat Piriform Cortex

(A_1–A_3) Baclofen abolishes ASSN-mediated synaptic transmission but has no effect on LOT-mediated fEPSPs. (A_1) Recording schematic. (A_2) LOT-mediated fEPSPs exhibit paired-pulse facilitation, whereas ASSN-mediated fEPSPs weakly depress. Cortical baclofen (500 μM) application abolishes the ASSN-mediated fEPSP while the LOT-mediated fEPSP is unaffected. (A_3) Summary (n = 4) of LOT (●) and ASSN (○) fEPSPs in response to baclofen and subsequent application of NBQX (50 μM). (B_1–B_3) Baclofen abolishes polysynaptic EPSCs and IPSCs but has no effect on monosynaptic LOT EPSCs. (B_1) Recording schematic. (B_2 and B_3) EPSCs (−80 mV) and IPSCs (+10 mV) evoked by LOT stimulation in the same cell before and during baclofen application. Dotted traces from control are superimposed. Grey boxes represent amplitude measurement regions that are plotted in (B_3) for IPSC (○) and monosynaptic EPSC (●). (C_1–C_5) Baclofen consistently blocks odor-evoked IPSCs but has variable effects on EPSCs, and the suppression of odor-evoked responses is reversed by subsequent application of a $GABA_B$ receptor antagonist. (C_1) Recording schematic. (C_2) Traces from one cell in response to odor presentation (2 s amyl acetate). Baclofen abolished odor-evoked IPSCs, whereas EPSCs were only partially blocked. (C_3) Fraction of the odor-evoked EPSC and IPSC blocked by baclofen for 27 odor-cell pairs (n = 7 cells). (C_4) Traces of (cineole) odor-evoked currents in one cell under control conditions (black), in the presence of baclofen (red), and following subsequent application of the antagonist CGP55845 (CGP, 10 μM, green). (C_5) Summary of the effects of baclofen (BAC) and CGP rescue on odor-evoked EPSC and IPSC charge normalized to control conditions (CON, n = 11 odor-cell pairs, n = 3 cells).

interneurons throughout the cortex (Bowery, 1993). However, brain slice studies have shown that although the $GABA_B$ receptor agonist baclofen abolishes ASSN-evoked excitatory transmission in APC, LOT-evoked excitatory responses are completely unaffected (Franks and Isaacson, 2005; Tang and Hasselmo, 1994). The absence of functional $GABA_B$ receptors on M/T cell nerve terminals suggests that baclofen could be a useful pharmacological tool to selectively silence intracortical excitatory synaptic input in vivo. In addition, local cortical application of baclofen should directly hyperpolarize APC pyramidal cells via postsynaptic $GABA_B$ receptors that are coupled to K^+ channels and should further reduce the likelihood of recurrent excitation (Bowery, 1993; Doi et al., 1990).

We therefore examined whether local cortical application of baclofen could be used to selectively silence intracortical excitation in vivo. We recorded field excitatory postsynaptic potentials (fEPSPs) in layer 1 of APC that were alternately evoked via stimulating electrodes placed in the LOT (afferent sensory pathway) and layer 2/3 (ASSN pathway; Figure 1A_1). Consistent with previous studies distinguishing the two pathways (Bower and Haberly, 1986; Franks and Isaacson, 2005; Poo and Isaacson, 2007), responses to paired-pulse stimulation (50 ms interval) were strongly facilitating for the LOT pathway (paired-pulse ratio [PPR] = 1.72 ± 0.18), but not the ASSN pathway (Figure 1A_2; PPR = 0.94 ± 0.07). In vivo cortical baclofen application (500 μM) rapidly abolished fEPSPs evoked by electrical stimulation of ASSN inputs (ASSN fEPSP slope 10 min post-baclofen 5% ± 10% of control; t test $p < 0.01$), whereas simultaneously recorded fEPSPs evoked by LOT stimulation were unaffected (Figures 1A_2 and 1A_3; LOT fEPSP slope 111% ± 14%; t test $p = 0.48$; n = 4 rats). Thus, activation of $GABA_B$ receptors in vivo selectively blocks intracortical excitatory synaptic transmission in APC.

We next studied the effects of baclofen in vivo using whole-cell voltage-clamp recording from layer 2/3 pyramidal cells (Poo and Isaacson, 2009). A cesium-based internal solution (5 mM Cl^-) was used to block K^+ channels and thus any direct action of baclofen in the recorded cell. A strong single pulse of LOT stimulation evoked short-latency, monosynaptic excitatory postsynaptic currents (EPSCs; $V_m = -80$ mV) and long-latency, polysynaptic EPSCs, reflecting the recruitment of intracortical excitation onto L2/3 pyramidal cells (Figure 1B_2). Interleaved trials at the reversal potential for EPSCs ($V_m = +10$ mV) revealed LOT-evoked inhibitory postsynaptic currents (IPSCs; Figure 1B_2)

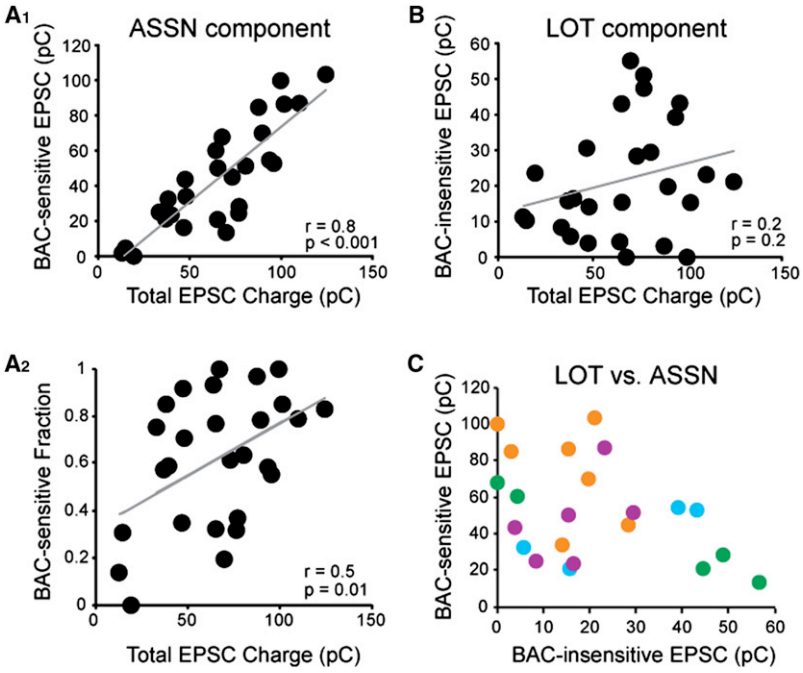

Figure 2. Contribution of Intracortical and Sensory-Afferent Inputs to Odor-Evoked Excitation in Piriform Cortex Pyramidal Cells

(A_1 and A_2) The strength of odor-evoked excitation is positively correlated with the recruitment of intracortical input. (A_1) Baclofen-sensitive charge (ASSN component) versus total EPSC charge for all odor-cell pairs with correlation (r) and p value. (A_2) Fraction of baclofen-sensitive charge (ASSN component) versus total EPSC charge for all odor-cell pairs. (B) Baclofen-insensitive charge (LOT component) is not correlated with odor-evoked excitation (total EPSC charge). (C) Within each cell, baclofen-sensitive (ASSN) excitatory responses are not correlated with the baclofen-insensitive (LOT) component. Each color represents odor-cell pairs from an individual cell (n = 4 cells that responded to $\geq$4/8 odors; Spearman's correlation, $p > 0.05$ for all cells).

that arise from local feedforward and feedback inhibitory circuits (Stokes and Isaacson, 2010). Baclofen abolished both polysynaptic EPSCs and IPSCs (Figure $1B_2$), consistent with the expression of presynaptic $GABA_B$ receptors on intracortical excitatory and inhibitory synapses (Bowery, 1993). However, monosynaptic LOT-evoked EPSCs simultaneously recorded onto the same cell were unaffected (Figures $1B_2$ and $1B_3$; n = 3 cells). Taken together, our experiments show that baclofen can be used in vivo to distinguish LOT- versus ASSN-mediated excitatory input onto an individual APC neuron, whereas the suppression of all IPSCs reports the effectiveness of baclofen at our recording site.

Determining the Contribution of ASSN versus LOT Inputs to Odor-Evoked Excitation

We next sought to determine the relative contribution of direct sensory and intracortical inputs to odor-evoked excitation in APC. To address this question, we used in vivo voltage-clamp recording to measure synaptic responses to a panel of eight structurally diverse monomolecular odorants in layer 2/3 pyramidal neurons (Figures $1C_1$–$1C_5$; Experimental Procedures; Poo and Isaacson, 2009). All cells included in this study were filled with biocytin for post hoc histological processing and were identified to be pyramidal in morphology (i.e., somata within deep layer 2 or layer 3, spiny apical dendrites extending to layer 1a, basal dendrites branching within layer 3; Suzuki and Bekkers, 2006). For each cell, we alternately monitored odor-evoked EPSCs and IPSCs before and after local cortical superfusion of baclofen (500 μM), and each odor-evoked response in a cell was considered an "odor-cell pair."

Cortical baclofen application strongly blocked odor-evoked IPSCs (Figures $1C_2$ and $1C_3$; mean fraction IPSC charge blocked = 0.93 ± 0.002; n = 27 odor-cell pairs), indicating the effectiveness of the drug at our recording site. On average, baclofen also suppressed odor-evoked EPSCs (Figures $1C_2$ and $1C_3$; mean fraction blocked = 0.49 ± 0.01). However, in contrast to the uniform suppression of odor-evoked IPSCs across all odor-cell pairs, baclofen had variable actions on odor-evoked excitation. For some odor-cell pairs, almost all excitation was blocked by baclofen, whereas for others excitation was largely unaffected (Figure $1C_3$). From these results, we conclude that, although the relative contribution of ASSN and LOT inputs could vary widely, both pathways participate in odor-evoked excitation. Furthermore, subsequent application of the $GABA_B$ receptor antagonist CGP55845 (CGP, 10 μM) to a subset of cells reversed the suppression of both excitatory and inhibitory synaptic currents, indicating the selective action of baclofen (Figures $1C_4$ and $1C_5$: n = 8 odor-cell pairs; n = 3 cells).

Intracortical Rather Than Sensory Inputs Underlie Strong Odor-Evoked Excitation

We quantified the intracortical ASSN contribution to odor-evoked EPSCs as the fraction of charge blocked by baclofen, while the fraction of charge remaining reflects the contribution of LOT inputs. Across all odor-cell pairs, we found that the strength of odor-evoked EPSCs was strongly correlated with the contribution of ASSN input (baclofen-sensitive EPSC; Figures $2A_1$ and $2A_2$). In other words, the most strongly driven responses were those reflecting the greatest amount of intracortical input, in terms of both absolute strength (Figure $2A_1$) and the fractional contribution to total excitation (Figure $2A_2$). In contrast, there was no significant correlation between the strength of odor-evoked EPSCs and the contribution of LOT sensory afferent input (Figure 2B). This lack of correlation between strength of LOT input and total excitation highlights the fact that odor-evoked responses of APC neurons do not simply reflect activity from converging M/T cell inputs. Specifically, our results indicate that intracortical rather than sensory afferent synapses underlie the most strongly driven odor-evoked synaptic excitation in APC.

In the sensory neocortex, intracortical and thalamocortical inputs onto individual neurons have been found to have similar preferences for sensory stimuli (Chung and Ferster, 1998; Liu et al., 2007). This implies that cortical circuitry, in which neurons receiving thalamocortical inputs with similar stimulus preferences excite each other, ultimately allows intracortical inputs to selectively amplify thalamocortical signals (Liu et al., 2007). We next considered whether there was evidence for this "cotuning" in APC based on the relationship between odor-evoked LOT- and ASSN-mediated excitation in individual cells. If intracortical circuits in APC selectively amplify afferent sensory input, the strength of ASSN-mediated excitation should be greatest for odor-cell pairs that receive the largest amount of LOT-mediated excitation. However, within individual cells responsive to multiple odors, the strength of LOT sensory input did not correlate with intracortical ASSN excitation (Figure 2C; n = 4 cells responsive to $\geq$4 out of 8 odors; Pearson's correlation $p > 0.1$). This lack of correlation held true when the strengths of ASSN and LOT inputs were rank ordered within each cell (Spearman's correlation $p > 0.05$). Thus, for individual cells, the relative contribution of ASSN and LOT inputs to responses to different odors varied widely. Similarly, there was no obvious relationship between the strength of ASSN and LOT input for responses to particular odorants across cells (see Figure S1 available online). Taken together, these results suggest that, unlike thalamorecipient neurons in the neocortex, intracortical excitation in APC does not arise from cotuned subcircuits of cortical neurons driven by common sensory input.

Intracortical Inputs Underlie Broadly Tuned Responses

How do intracortical and direct sensory inputs shape the excitatory responses of an individual APC pyramidal cell to different odors? In other words, how do intracortical and direct sensory inputs contribute to the "tuning" of excitatory responses (EPSC tuning)? Odor-evoked excitation onto most pyramidal cells is relatively selective (responses to one or two out of eight test odors), but some neurons are broadly tuned to multiple odors (Poo and Isaacson, 2009; Zhan and Luo, 2010). EPSC tuning was determined by categorizing excitation as "responsive" versus "nonresponsive" (Poo and Isaacson, 2009), as measured from the increase in charge transfer during odor presentation (see Experimental Procedures). We observed marked differences in the actions of baclofen on odor-evoked excitation that was related to the EPSC tuning of individual cells. In pyramidal cells that were selectively excited, odor-evoked EPSCs were only moderately suppressed in the presence of baclofen (Figures 3A_1 and 3A_2). In contrast, odor-evoked EPSCs were strongly blocked in cells that responded broadly to multiple odors (Figures 3B_1 and 3B_2). Reconstruction of the pyramidal cells receiving selective or broadly tuned excitation revealed similar anatomical features, such as somatic location and dendritic arborization (Figures 3A_1 and 3B_1). Odor-evoked inhibition is broadly tuned in APC pyramidal cells, irrespective of the tuning of excitation in the same cells (Poo and Isaacson, 2009). Baclofen uniformly abolished odor-evoked IPSCs in cells that received either selective or broadly tuned excitation (Figures 3A_2 and 3B_2), ruling out the possibility that its different actions on excitation reflected differences in access of the drug to the local circuit. These results suggest that intracortical inputs might dominate odor-evoked excitation in broadly tuned neurons yet contribute relatively weakly to excitation in selectively responsive cells.

We further quantified the relationship between EPSC tuning observed under control conditions and the contribution of ASSN and LOT input assessed following baclofen application. Cells tested with baclofen (n = 7) encompassed a wide range of EPSC tuning properties, from selective (responses to 1/8 tested odors, i.e., Figure 3A_2) to broad (responses to 7/8 odors, i.e., Figure 3B_2). We found that the strength and fractional contribution of baclofen-sensitive intracortical excitation for each odor response was positively correlated with the EPSC tuning properties of the cell (Figures 4A_1 and 4A_2). This suggests that broadly tuned cells received greater amounts of ASSN-mediated excitation than selective cells. In contrast, both selective and broadly tuned cells received similar amounts of excitation from LOT afferents (Figure 4B). Averaging the ASSN and LOT components across odor-evoked responses within each cell yielded similar results (data not shown). Furthermore, broadly tuned neurons received greater amounts of total excitatory synaptic input (Figure 4C), consistent with the fact that the strength of odor-evoked excitatory responses is correlated with ASSN input (i.e., Figure 2A_1).

Comparing the responsiveness of the cell population to odors before and after baclofen application revealed the importance of ASSN inputs to EPSC tuning. In cells responding to multiple odors, baclofen reduced the number of odors eliciting excitation (Figure 4D), indicating an increase in odor selectivity. We also determined the effect of baclofen on selectivity using lifetime sparseness (S_L, ranging from 0 = nonselective to 1 = highly selective), a measure of how an individual cell responds to multiple stimuli that does not rely on binary categorization of responses (Willmore and Tolhurst, 2001). Across the cell population, this analysis of EPSC charge also revealed that silencing ASSN inputs caused a significant increase in odor selectivity (control $S_L = 0.33 \pm 0.16$, baclofen $S_L = 0.59 \pm 0.16$, $p = 0.02$). Thus, the net effect of removing intracortical inputs is to make broadly tuned pyramidal cells more selective.

DISCUSSION

In this study, we used in vivo whole-cell voltage-clamp recordings to show that intracortical excitatory inputs play an important role in shaping odor-evoked synaptic excitation in the piriform cortex. We took advantage of the distinct properties of synaptic circuits in the olfactory cortex and selectively silenced intracortical synapses via $GABA_B$ receptor activation. We found that strongly driven odor-evoked excitatory synaptic responses largely reflect the contribution of intracortical ASSN inputs. Furthermore, the relative contribution of direct sensory LOT input and intracortical input to odor-evoked excitation varies with the tuning properties of individual pyramidal cells. Specifically, broadly tuned cells receive stronger intracortical excitation, whereas cells that respond selectively to odors receive mainly afferent sensory input.

LOT afferent fibers target the distal portion of pyramidal cell apical dendrites in layer 1a, whereas associational synapses contact more proximal apical dendrites in layer 1b, as well as

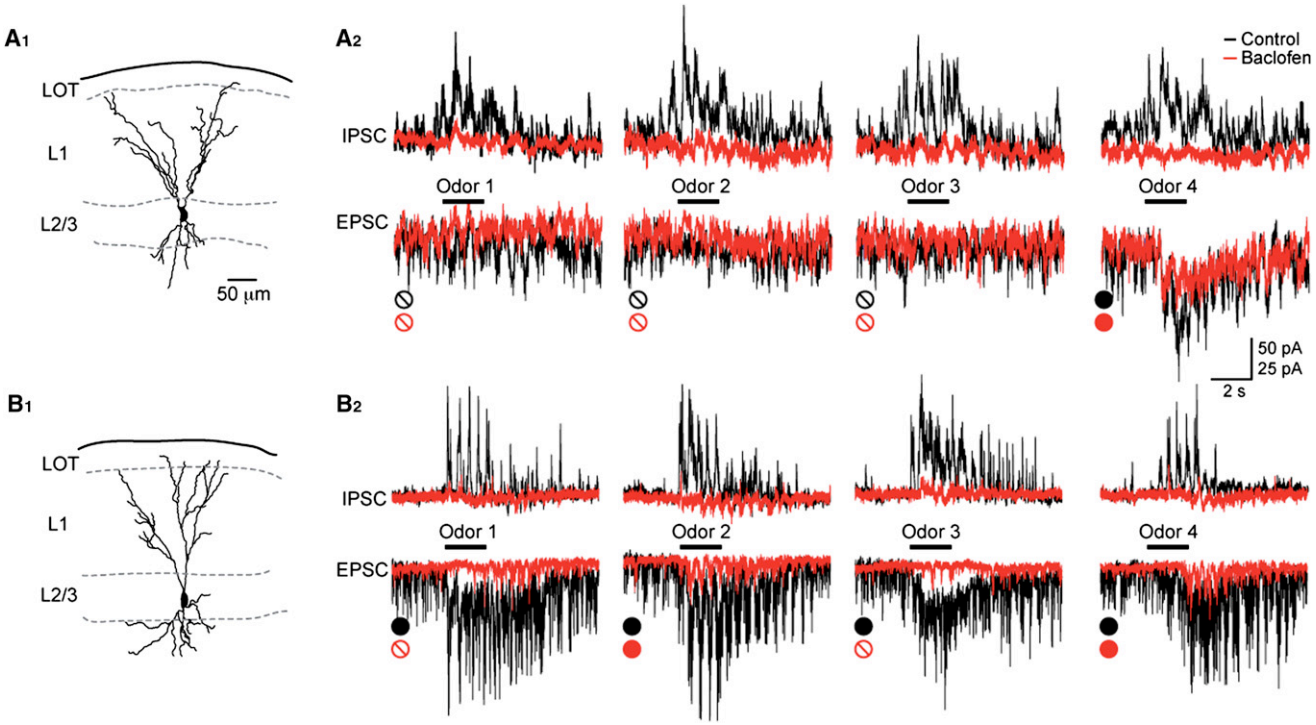

Figure 3. Silencing Intracortical Inputs Has Different Effects on Odor-Evoked Excitation Depending on the EPSC Tuning Properties of Individual Cells

(A_1 and A_2) Baclofen has weak effects on odor-evoked EPSCs in cells that receive selective excitation. Anatomical reconstruction (A_1) and synaptic responses (A_2) illustrate a representative pyramidal cell that received broadly tuned odor-evoked inhibition (IPSCs, +10 mV) and selective excitation (EPSCs, −80 mV). Under control conditions (black), one out of eight odorants elicited excitation, which was largely unaffected by baclofen (red). For display purposes, only four odor responses are shown. ● represents significant odor response; ⊘ represents lack of response (see Experimental Procedures). Scale bars represent 50 pA for IPSCs, 25 pA for EPSCs. (B_1 and B_2) Baclofen strongly blocks odor-evoked EPSCs in cells receiving broadly tuned excitation. Anatomy (B_1) and synaptic responses (B_2) illustrate a representative cell that received widespread inhibition and broadly tuned excitation. Seven out of eight odorants elicited excitation under control conditions (four odors displayed). Same scale as in (A_2). Odors 1–4 were as follows: cineole, amyl acetate, (R)-limonene, and phenylethyl alcohol.

basal dendrites of pyramidal cells in layers 2/3 (Neville and Haberly, 2004). How valid are our somatic recordings of EPSC charge for determining the relative impact of LOT and ASSN inputs to pyramidal cell excitability? LOT-mediated EPSCs might be more heavily attenuated than proximal ASSN EPSCs at our somatic recording location due to dendritic filtering. However, the dendrites of piriform cortex pyramidal cells are relatively electrotonically compact, with only a 50% maximal somatic current loss for synaptic inputs arriving at the most distal dendritic regions (Bathellier et al., 2009). In addition, piriform pyramidal cell dendrites are only weakly active, and spike output has been shown to reflect the nearly linear summation of synaptic inputs at the soma of these cells (Bathellier et al., 2009). Together, these findings suggest that our somatic charge measurements are a good indicator of the excitation that triggers spike output of piriform pyramidal cells.

Recent studies have shown how the convergence and integration of M/T cell inputs from different glomeruli onto piriform cortical neurons can shape odor representations in the piriform cortex (Apicella et al., 2010; Davison and Ehlers, 2011; Miyamichi et al., 2011). However, in addition to olfactory bulb afferent input patterns, excitatory intracortical input has also been suggested to shape response properties of piriform cortical neurons. Indeed, experiments in APC slices revealed extensive long-range recurrent connections and suggest that individual pyramidal cells receive far larger numbers of recurrent inputs than afferent inputs (Franks et al., 2011 [this issue of *Neuron*]). Furthermore, in vivo intracellular recordings from APC neurons found that excitatory postsynaptic potentials (EPSPs) could be evoked in cells by costimulation of multiple glomeruli, even when activation of the individual glomeruli alone did not produce detectable EPSPs (Davison and Ehlers, 2011). This supralinear recruitment of excitation implies an indirect source of synaptic input consistent with intracortical circuits.

Our results provide evidence for an extensive functional contribution of intracortical excitatory inputs to odor-evoked excitation in the piriform cortex. Similarly, intracellular recordings from thalamorecipient neurons in the primary visual and auditory cortex have shown that intracortical inputs can underlie a substantial component of sensory-evoked excitation (Chung and Ferster, 1998; Liu et al., 2007). However, unlike neurons in the sensory neocortex (Liu et al., 2007), we found that the

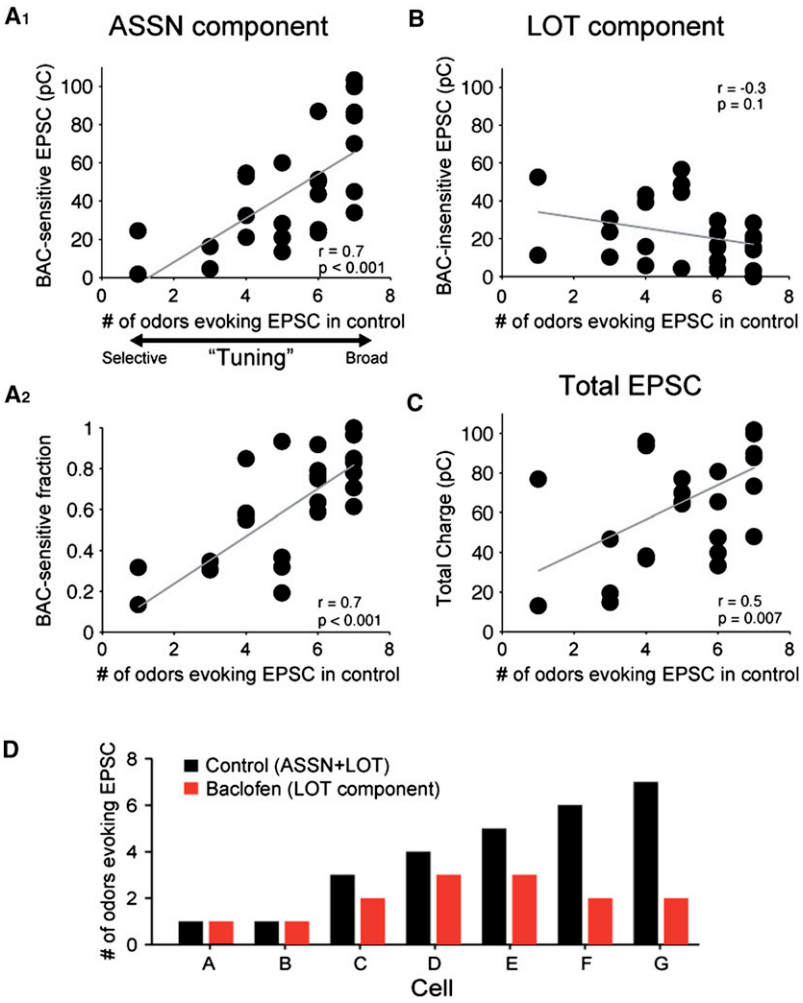

Figure 4. Intracortical Inputs Underlie Broadly Tuned Odor-Evoked Excitation in Piriform Cortex

(A_1–A_2) Broadly tuned cells receive stronger intracortical input than selectively responding cells. (A_1) A strong correlation between EPSC tuning and the baclofen-sensitive charge (ASSN) component of EPSCs across all odor-cell pairs. (A_2) The baclofen-sensitive (ASSN) fraction of odor-evoked excitation displays a similar strong correlation with EPSC tuning. (B) The baclofen-insensitive (LOT) charge component of odor-evoked excitation in the same cells is not correlated with EPSC tuning. (C) The strength of odor-evoked excitation (total charge) is positively correlated with EPSC tuning. In (A)–(C), n = 27 odor-cell pairs, n = 7 cells. (D) Blocking intracortical input increases the selectivity of odor-evoked excitation for broadly tuned neurons, while narrowly tuned cells are unaffected.

strength of intracortical excitation was not related to the amount of afferent sensory input recruited by the same stimulus in individual cells. Thus, strong intracortical excitation could be produced in APC neurons by stimuli that evoked only very weak direct sensory input. This apparent lack of cotuning suggests that intracortical circuits in APC have a different organization than those that selectively amplify thalamocortical inputs in the neocortex.

We also found that the contribution of intracortical connections and sensory inputs to excitation differed based on the tuning properties of individual cells. Recent slice studies have suggested that layer 2 principal APC cells fall into two classes in terms of their excitatory inputs: semilunar cells in layer 2a that lack basal dendrites and are proposed to receive strong LOT input and weak ASSN input and pyramidal cells in layer 2b that receive weaker LOT input but strong ASSN input (Suzuki and Bekkers, 2006, 2011). Semilunar and pyramidal cells might thus differentially process afferent and associational inputs and possess different tuning properties (selective and broad, respectively). One possibility is that the differences we find for the contribution of intracortical inputs to odor responses reflect these two cell classes. However, none of the cells we recorded were located in superficial layer 2a, and all had basal dendrites, suggesting that all of the cells we studied were layer 2/3 pyramidal cells. Furthermore, a recent in vivo extracellular recording study also found that the response properties of identified layer 2/3 pyramidal cells could be classified as selective or broadly tuned for a large panel of odors (Zhan and Luo, 2010).

In summary, we provide direct evidence for a significant role of intracortical inputs to odor-evoked excitation in the olfactory cortex. Our results illustrate that intracortical connections in APC expand the range of odors over which pyramidal cells can respond and that odor tuning does not simply reflect varying degrees of M/T cell convergence onto individual cells. Intracortical connections are likely to underlie the distributed and dynamic nature of cortical odor representations and are poised to play a role in associative processes such as pattern completion and olfactory learning (Barnes et al., 2008; Haberly, 2001; Rennaker et al., 2007; Roesch et al., 2007; Stettler and Axel, 2009).

EXPERIMENTAL PROCEDURES

All experiments were performed in accordance with the guidelines of the National Institutes of Health and the University of California Institutional Animal Care and Use Committee. Sprague Dawley rats (16–21 days old) were anesthetized with urethane (1.5 g/kg) and maintained at 35°C–37°C. A small (~1 mm^2) craniotomy was made lateral to the rhinal sulcus and dorsal to the top edge of the LOT to expose the APC, and the cortical surface was constantly superfused with warmed (34°C) artificial cerebral spinal fluid (aCSF) containing 119 mM NaCl, 2.5 mM KCl, 2.5 mM $CaCl_2$, 1.3 mM $MgSO_4$, 1 mM NaH_2PO_4, 26.2 mM $NaHCO_3$, and 22 mM glucose, equilibrated with 95% O_2 and 5% CO_2.

Odors (cineole, amyl acetate, (R)-limonene, phenylethyl alcohol, eugenol, dimethyl pyrzadine, citral, and ethyl butyrate) were delivered at a concentration of 5% saturated vapor via a computer-controlled olfactometer in pseudorandomized order for 2 s, with 60 s between presentations of odors.

In vivo whole-cell recordings were made using pipettes (5–7 MΩ) containing 130 mM cesium gluconate, 5 mM NaCl, 10 mM HEPES, 0.2 mM EGTA, 12 mM

phosphocreatine, 3 mM Mg-ATP, 0.2 mM Na-GTP, and biocytin (0.2% mM). EPSCs were recorded at −80 mV, the reversal potential (E_{rev}) for inhibition set by our internal solution. Similarly, IPSCs were recorded at E_{rev} for excitation (~+10 mV). We determined the adequacy of voltage-clamp recordings by ensuring that inward EPSCs recorded at −80 mV were abolished at a holding potential of +10 mV (cf. LOT-evoked monosynaptic EPSC in Figures $1B_1$–$1B_3$). This was consistently achieved when series resistance (R_s) was ≤30 MΩ. R_s was continuously monitored during each recording to rule out the possibility that changes in synaptic responses reflected gradual increases in R_s. Cells in which R_s changed by >15% were excluded (R_s control: 24.3 ± 2.3 MΩ; R_s baclofen: 26.0 ± 3.2 MΩ; paired t test, p = 0.09; n = 7). Furthermore, there was no correlation between R_s and EPSC tuning (r = 0, p = 0.98) or strength of odor-evoked synaptic excitation (r = 0.2, p = 0.6). fEPSPs were recorded with an aCSF-filled pipette (1 MΩ) placed ~100 μm below the pial surface.

Recordings were made with a MultiClamp 700A (Molecular Devices) and AxoGraph X. Data were analyzed using custom routines in MATLAB (Mathworks). Cells were analyzed only if >4 odor presentation trials for control and drug conditions were obtained. Odor-evoked synaptic activity was aligned to the onset of the first inspiration in the presence of odor and was quantified by calculating charge transfer (Q_{Odor}) during the 2 s odor period. Baseline response ($Q_{Baseline}$) was calculated from a 2 s period preceding odor onset. The criteria for a "positive" odor-evoked synaptic response was defined as response index = ($Q_{Odor}/Q_{Baseline}$) ≥ 1.6. This threshold was derived from receiver-operating characteristic analysis to obtain the optimal threshold that produced a true-positive to false-positive ratio of >90% (Poo and Isaacson, 2009). Lifetime sparseness (S_L), which is independent of detection threshold, was calculated as $(1 - \{[S^N_j\ r_j/N]^2/\{S^N_j\ [r_j^2/N]\}\})/(1 - 1/N)$, where r_j was the response of the neuron to odorant j (charge transfer) and N was the total number of odors (Willmore and Tolhurst, 2001).

SUPPLEMENTAL INFORMATION

Supplemental Information includes one figure and can be found with this article online at doi:10.1016/j.neuron.2011.08.015.

ACKNOWLEDGMENTS

We are grateful to M. Scanziani for helpful comments and P. Abelkop for technical assistance. Supported by R01DC04682 (J.S.I.) and 5F31DC009366 (C.P.).

Accepted: August 8, 2011
Published: October 5, 2011

REFERENCES

Apicella, A., Yuan, Q., Scanziani, M., and Isaacson, J.S. (2010). Pyramidal cells in piriform cortex receive convergent input from distinct olfactory bulb glomeruli. J. Neurosci. *30*, 14255–14260.

Barnes, D.C., Hofacer, R.D., Zaman, A.R., Rennaker, R.L., and Wilson, D.A. (2008). Olfactory perceptual stability and discrimination. Nat. Neurosci. *11*, 1378–1380.

Bathellier, B., Margrie, T.W., and Larkum, M.E. (2009). Properties of piriform cortex pyramidal cell dendrites: implications for olfactory circuit design. J. Neurosci. *29*, 12641–12652.

Bower, J.M., and Haberly, L.B. (1986). Facilitating and nonfacilitating synapses on pyramidal cells: a correlation between physiology and morphology. Proc. Natl. Acad. Sci. USA *83*, 1115–1119.

Bowery, N.G. (1993). $GABA_B$ receptor pharmacology. Annu. Rev. Pharmacol. Toxicol. *33*, 109–147.

Chung, S., and Ferster, D. (1998). Strength and orientation tuning of the thalamic input to simple cells revealed by electrically evoked cortical suppression. Neuron *20*, 1177–1189.

Davison, I.G., and Ehlers, M.D. (2011). Neural circuit mechanisms for pattern detection and feature combination in olfactory cortex. Neuron *70*, 82–94.

Doi, N., Carpenter, D.O., and Hori, N. (1990). Differential effects of baclofen and gamma-aminobutyric acid (GABA) on rat piriform cortex pyramidal neurons in vitro. Cell. Mol. Neurobiol. *10*, 559–564.

Franks, K.M., and Isaacson, J.S. (2005). Synapse-specific downregulation of NMDA receptors by early experience: a critical period for plasticity of sensory input to olfactory cortex. Neuron *47*, 101–114.

Franks, K.M., Russo, M.J., Sosulski, D.L., Mulligan, A.A., Siegelbaum, S.A., and Axel, A. (2011). Recurrent circuitry dynamically shapes the activation of piriform cortex. Neuron *72*, this issue, 49–56.

Ghosh, S., Larson, S.D., Hefzi, H., Marnoy, Z., Cutforth, T., Dokka, K., and Baldwin, K.K. (2011). Sensory maps in the olfactory cortex defined by long-range viral tracing of single neurons. Nature *472*, 217–220.

Haberly, L.B. (2001). Parallel-distributed processing in olfactory cortex: new insights from morphological and physiological analysis of neuronal circuitry. Chem. Senses *26*, 551–576.

Haberly, L.B., and Price, J.L. (1978). Association and commissural fiber systems of the olfactory cortex of the rat. J. Comp. Neurol. *178*, 711–740.

Illig, K.R., and Haberly, L.B. (2003). Odor-evoked activity is spatially distributed in piriform cortex. J. Comp. Neurol. *457*, 361–373.

Johnson, D.M., Illig, K.R., Behan, M., and Haberly, L.B. (2000). New features of connectivity in piriform cortex visualized by intracellular injection of pyramidal cells suggest that "primary" olfactory cortex functions like "association" cortex in other sensory systems. J. Neurosci. *20*, 6974–6982.

Liu, B.H., Wu, G.K., Arbuckle, R., Tao, H.W., and Zhang, L.I. (2007). Defining cortical frequency tuning with recurrent excitatory circuitry. Nat. Neurosci. *10*, 1594–1600.

Miyamichi, K., Amat, F., Moussavi, F., Wang, C., Wickersham, I., Wall, N.R., Taniguchi, H., Tasic, B., Huang, Z.J., He, Z., et al. (2011). Cortical representations of olfactory input by trans-synaptic tracing. Nature *472*, 191–196.

Poo, C., and Isaacson, J.S. (2007). An early critical period for long-term plasticity and structural modification of sensory synapses in olfactory cortex. J. Neurosci. *27*, 7553–7558.

Poo, C., and Isaacson, J.S. (2009). Odor representations in olfactory cortex: "sparse" coding, global inhibition, and oscillations. Neuron *62*, 850–861.

Rennaker, R.L., Chen, C.F., Ruyle, A.M., Sloan, A.M., and Wilson, D.A. (2007). Spatial and temporal distribution of odorant-evoked activity in the piriform cortex. J. Neurosci. *27*, 1534–1542.

Roesch, M.R., Stalnaker, T.A., and Schoenbaum, G. (2007). Associative encoding in anterior piriform cortex versus orbitofrontal cortex during odor discrimination and reversal learning. Cereb. Cortex *17*, 643–652.

Rubin, B.D., and Katz, L.C. (1999). Optical imaging of odorant representations in the mammalian olfactory bulb. Neuron *23*, 499–511.

Sosulski, D.L., Bloom, M.L., Cutforth, T., Axel, R., and Datta, S.R. (2011). Distinct representations of olfactory information in different cortical centres. Nature *472*, 213–216.

Soucy, E.R., Albeanu, D.F., Fantana, A.L., Murthy, V.N., and Meister, M. (2009). Precision and diversity in an odor map on the olfactory bulb. Nat. Neurosci. *12*, 210–220.

Stettler, D.D., and Axel, R. (2009). Representations of odor in the piriform cortex. Neuron *63*, 854–864.

Stokes, C.C., and Isaacson, J.S. (2010). From dendrite to soma: dynamic routing of inhibition by complementary interneuron microcircuits in olfactory cortex. Neuron *67*, 452–465.

Suzuki, N., and Bekkers, J.M. (2006). Neural coding by two classes of principal cells in the mouse piriform cortex. J. Neurosci. *26*, 11938–11947.

Suzuki, N., and Bekkers, J.M. (2011). Two layers of synaptic processing by principal neurons in piriform cortex. J. Neurosci. *31*, 2156–2166.

Tang, A.C., and Hasselmo, M.E. (1994). Selective suppression of intrinsic but not afferent fiber synaptic transmission by baclofen in the piriform (olfactory) cortex. Brain Res. *659*, 75–81.

Uchida, N., Takahashi, Y.K., Tanifuji, M., and Mori, K. (2000). Odor maps in the mammalian olfactory bulb: domain organization and odorant structural features. Nat. Neurosci. *3*, 1035–1043.

Wachowiak, M., and Cohen, L.B. (2001). Representation of odorants by receptor neuron input to the mouse olfactory bulb. Neuron *32*, 723–735.

Willmore, B., and Tolhurst, D.J. (2001). Characterizing the sparseness of neural codes. Network *12*, 255–270.

Wilson, D.A. (2001). Receptive fields in the rat piriform cortex. Chem. Senses *26*, 577–584.

Zhan, C., and Luo, M. (2010). Diverse patterns of odor representation by neurons in the anterior piriform cortex of awake mice. J. Neurosci. *30*, 16662–16672.